10TH INTERNATIONAL SYMPOSIUM ON PARTICLE IMAGE VELOCIMETRY - PIV13
Delft, The Netherlands, July 1-3, 2013

Characterization of the Interaction between Tollmien-Schlichting Waves and a DBD Plasma Actuator using Phase-locked PIV

A. Widmann, A. Kurz, B. Simon, S. Grundmann, C. Tropea

Center of Smart Interfaces, Technische Universität Darmstadt, GERMANY
widmann@sla.tu-darmstadt.de, kurz@csi.tu-darmstadt.de

ABSTRACT

The research reported in this study addresses the direct measurement of Tollmien-Schlichting (TS) waves on a flat plate, when the laminar boundary layer is excited by velocity perturbations. Tollmien-Schlichting waves are a precursor to natural laminar-to-turbulent transition and, if these waves can be reduced in amplitude, a transition delay can be realized, resulting in lower overall friction drag. One such means of actively suppressing TS waves is the application of dielectric barrier discharge (DBD) plasma actuators [2]. These devices can be operated in several different modes to achieve a decrease of TS-wave amplitude and the physics of the actuator/wave interaction differs for each mode. In the present study two particular modes are investigated; the boundary-layer stabilization mode, in which the actuator is operated continuously (quasi-steady); and the hybrid mode, in which the actuator amplitude is modulated about a steady value. The purpose of the present measurements is to demonstrate the feasibility of measuring the DBD actuator interaction with the TS-waves using phase-locked Particle Image Velocimetry. Obtaining such velocity field data in the interaction zone of the DBD actuator allows insight into the physics of the actuator/TS-wave interaction. However the measurements are particular challenging, since the amplitude of TS-waves in their linear growth region is typically less than 1% of the freestream velocity; therefore some particular remarks about the PIV data processing will be directed towards achieving the necessary accuracy and resolution.

1. Introduction

The transition from a laminar to a turbulent boundary layer for flows under low disturbance conditions is caused by instabilities of the boundary layer. These instabilities occur according to Schlichting and Gersten [1], when the Reynolds number Re of the flow is large enough to exceed the so called indifference Reynolds-number Re_{ind}. Beyond this point small disturbances are amplified and destabilize the boundary layer. Initially these disturbances form a wave-like flow pattern, known as Tollmien-Schlichting (TS) waves. These waves are two-dimensional, periodic velocity fluctuations, whose amplitude grows in the downstream direction. As their amplitude grows, these waves become three-dimensional and start to form vortices, which subsequently break up and form single turbulent spots in the boundary layer. These spots then develop into a fully turbulent flow. Because of their defined structure (compared to later stages of boundary layer transition) and their periodic behavior, TS waves can be relatively easily manipulated. If the amplitudes of the TS waves are locally reduced, their growth is delayed and so are all subsequent stages of the transition. By this means the laminar-to-turbulent transition can be delayed. The benefit of such a transition delay lies in reduced drag, because turbulent boundary layers exhibit significantly higher values of skin friction than laminar boundary layers.

Our research at the Technische Universität Darmstadt focuses on plasma actuators (PA) as a controlling device for transition delay. When TS waves pass over a plasma actuator, its body force can interact with the TS waves in such a manner, that their amplitude is reduced. The two fundamental mechanisms for attenuating the amplitude of TS waves are the active wave cancelation [2] and the boundary-layer stabilization [3]. For achieving a boundary-layer stabilization a quasi-steady body force is used. By inducing momentum into the boundary layer, it's stability characteristics are modified such that the existing perturbations are dampened indirectly by the more stable boundary-layer velocity profile. In the case of active wave cancelation the body force acts directly on the velocity fluctuations of the wave. To achieve this, an unsteady body force is produced to directly counteract the velocity fluctuations. This more complicated procedure requires an active control system, as previously applied by Kurz [4]. The exact interaction of the body force and the waves for both fundamentally different wave attenuation mechanisms has not yet been investigated in great detail, because data inside the body force field are not available with conventional measurement techniques. Since the plasma actuator operates at high voltages, electromagnetic interference is introduced to hot-wire probe signals when they are placed in the vicinity of the actuator. Therefore an optical measurement technique is necessary for gaining insight into the wave/actuator interactions. This study demonstrates the feasibility of Particle Image Velocimetry (PIV) to resolve TS waves and to quantify the dampening effects of the plasma actuator.

PIV was chosen, because it captures a two-dimensional field of view (FOV) and is able to reveal the interplay of wall-normal and wall-parallel velocity fluctuations caused by TS waves and to resolve their structures. The challenges in measuring TS waves using PIV lies in their small velocity amplitude superimposed on a mean velocity, two orders of magnitude higher. Because their structure extends beyond the outer edge of the boundary layer, the FOV has to capture at least a small part of the free stream flow above the boundary-layer edge. Therefore large velocity gradients will be present in the acquired data. Concerning the wall-parallel extension of the FOV, it is

desirable to capture at least one entire TS wavelength, which would require the FOV to be large. Concerning the wall-normal extension of the FOV the near-wall region should be resolved as fine as possible . A compromise of these conflicting requirements has to be found. In the present study the wave attenuation effect achieved by a pure boundary-layer stabilization and caused by a hybrid operating mode (combination of boundary-layer stabilization and wave cancelation) has been investigated to demonstrate the feasibility of the PIV technique.

2. Experimental Setup

2.1 General Setup

All experiments were carried out in the Eiffel type wind tunnel at Technische Universität Darmstadt. The following description of the setup and the data acquisition has been taken from [5], where a similar setup was used. The wind tunnel has a cross section of $0,45\,m\,x\,0,45\,m$ with an inlet contraction ratio of $24:1$. A flat plate with an elliptical leading edge and a total length of $L_{total} = 1600\,mm$ is placed inside the tunnel at a free stream velocity of $U_\infty = 16\,\frac{m}{s}$. The TS waves are excited with a disturbance source consisting of a vibrating ribbon flush-mounted to the flat plate, it is placed at a distance of $L_{ds} = 230\,mm$ downstream of the leading edge, the plasma actuator is placed at a distance of $L_{ds-pa} = 120\,mm$ downstream of the disturbance source. A flap at the flat plate's trailing edge ensures a negligible pressure gradient across the flat plate and keeps the stagnation point of the incoming flow on the upper surface of the flat plate. Boundary-layer separation and bypass transition are prevented. The setup is illustrated in Figure 1. The center of the FOV and the laser light sheet are placed at a distance $L_{FOV} = 60\,mm$ downstream the plasma actuator. During all experiments the most unstable excitation frequency according to linear stability theory was chosen, which results in the strongest growth of TS waves. For a free stream velocity of $U_\infty = 16\,\frac{m}{s}$ the disturbance source was operated at a frequency of $f_{ds} = 250\,Hz$.

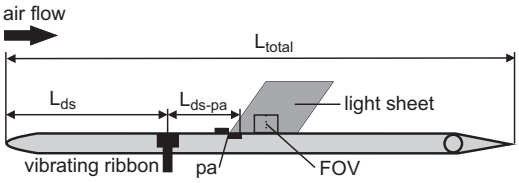

Figure 1: Setup of the flat plate including disturbance source, plasma actuator and FOV

2.2 Plasma Actuator and Operation Modes

The working principle of a DBD plasma actuator is based on an unsteady electric field between two electrodes supplied with a radio frequency voltage of several kilo Volt amplitude. The two electrodes are separated by a dielectric material as illustrated in Figure 2. If an alternating high voltage of order 10kV is applied, air molecules become ionized and are accelerated by the electric field. Collisions of charged particles with neutral air molecules lead to a momentum transfer that appears as a body force tangential to the wall.

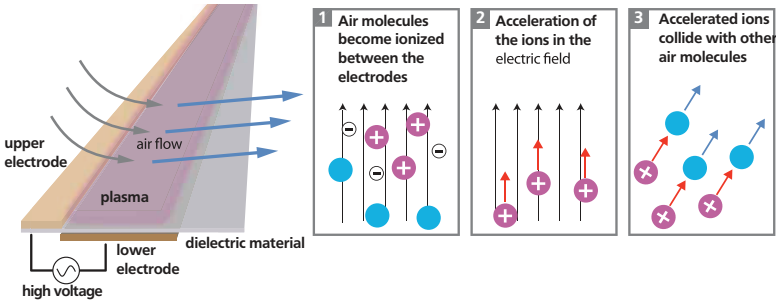

Figure 2: Working principle of a DBD plasma actuator

In this manuscript two different approaches for achieving a transition delay are discussed: the pure boundary-layer stabilization and a hybrid operation mode, comprising boundary-layer stabilization and active wave cancelation in one single actuator. Experimental results of both operating modes are compared to a reference case without active control. For this reference case only the disturbance source operates to excite the TS waves.

In the boundary-layer stabilization mode the actuator creates a quasi-steady body force in the downstream direction (Figure 3(a)), which feeds momentum into the boundary layer, changes its velocity profile and thereby manipulates its stability properties. The TS waves experience lower amplification or even an attenuation due to the modified velocity profile. This results in smaller amplitudes at a given position downstream of the plasma actuator. Due to the changes in the stability properties of the boundary layer, different convective speeds and/or wavelengths for the excited disturbances at the fixed frequency can be expected with respect to the reference case. Since the modification of velocity profile decays as the flow travels downstream, the dampening effect due to reduced amplification rates is expected to be distributed over some wavelengths downstream of the plasma actuator and to also decay.

The second operation mode combines the two fundamental mechanisms to attenuate TS waves using a plasma actuator. Active wave

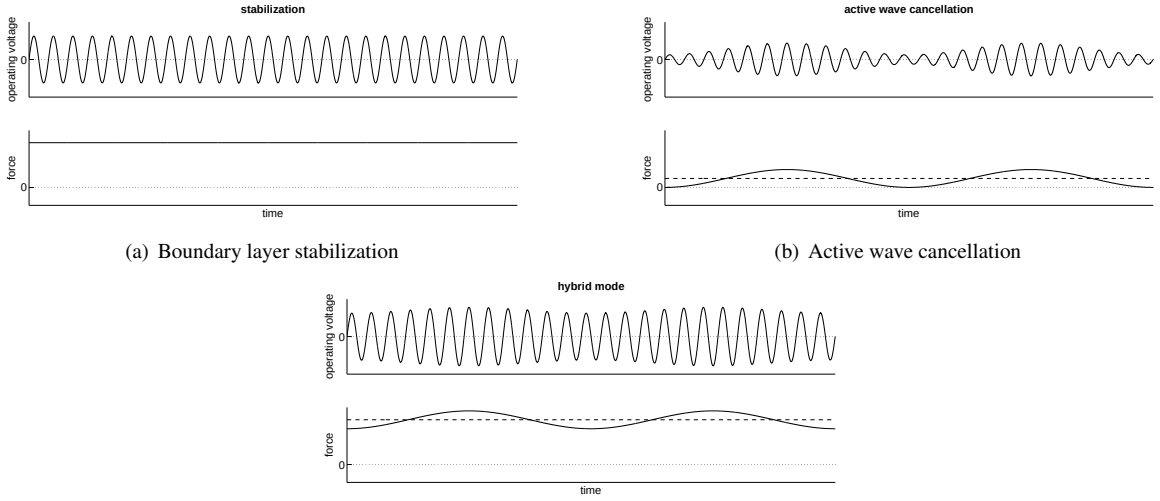

(a) Boundary layer stabilization

(b) Active wave cancellation

(c) Hybrid operation mode

Figure 3: Plasma actuator operation modes

cancelation (Figure 3(b)) is combined with the boundary stabilization to a new hybrid operation mode (Figure 3(c)). The quasi-steady force stabilizes the boundary layer as described above and is superimposed with an alternating part, which directly counteracts the velocity deviations caused by the wave to cancel them out. Because of the force offset, the actuator can counteract positive as well as negative velocity deviations of the wave whereas the AWC mode only enables forcing in one direction. As energy savings are the motivation for the drag reduction, the new hybrid operation mode is promising. It adds the effect of the active wave cancelation to the boundary-layer stabilization with no additional net power.

2.3 Controller System

In active wave cancelation and hybrid operation mode the amplitude and phase of the actuator force should be adjusted by a controller. For the current setup a filtered x-LMS controller, developed by Baumann [6], is used for TS wave damping. The plasma actuator is operated by a Minipuls 2.1 at a frequency of 11 kHz. This high voltage generator allows to modulate the amplitude of the output voltage via an analog input signal of 0-5V. Two surface hot wires, operated by a DISA 55M01 constant temperature anemometer, serve as reference and error sensor for the controller while the computational power is provided by an dSpace (DS1006) digital signal processor.

2.4 Data Acquisition

PIV offers advantages for measuring the interaction of plasma actuators with TS waves, but some challenges remain. Typically the magnitudes of the measured velocity deviations are of the order of 1% of the free stream velocity. Stochastic velocity fluctuations in the wind tunnel may be of the same order of magnitude, especially near the wall, and can mask the structure of the waves. An averaging procedure is necessary to extract the periodic waves from the statistic noise. Because the structure of the TS waves extends from the wall to regions in the free stream, the PIV system has to accurately measure small velocity deviations in a large velocity range. Additionally the frequency of the TS waves is orders of magnitude higher than the repetition rate of the available PIV system. These circumstance require a triggering of the PIV system to fixed phase angles of the periodic TS-waves, i.e. to the excitation signal. A repeated measurement at the same phase angle and a subsequent ensemble averaging filters out the stochastic effects overlaid to the TS waves. To obtain statistical convergence a sufficient number of image pairs is necessary.
The implementation of the coupling between image acquisition and phase angle is given in Figure 4. A continuous sinusoidal excitation signal controls the motion of the vibrating ribbon. For a fixed excitation frequency and a fixed free stream velocity, the TS wave convection speed remains constant. In combination with the fixed distance between FOV and the disturbance source the convection speed of the TS wave results in a fixed temporal delay or phase shift between excitation and acquisition.

A delay generator establishes the connection between excitation signal and data acquisition. The delay generator detects a transgression of the excitation voltage over a threshold and sends a trigger signal to the PIV system. By increasing this time delay, data of arbitrary phase angles Φ can be acquired. Figure 5 depicts the timing diagram schematically.

For the same phase angle Φ 1700 image pairs are acquired and merged into one ensemble. All twelve ensembles can be combined to reconstruct the whole average cycle of the TS wave. For the presented experiments the ensembles correspond to wave phases of $\Phi = [0^\circ\ 30^\circ\ 60^\circ\ ...\ 330^\circ]$. This data acquisition procedure is the same for all measurement cases (reference case, boundary layer stabilization, hybrid mode).

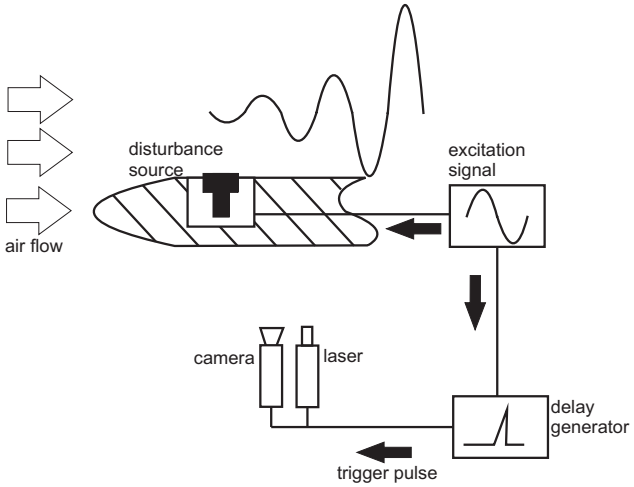

Figure 4: Phase coupling between the excitation signal and the image acquisition of the PIV system using a delay generator

Single camera setup - reference case and boundary-layer stabilization:

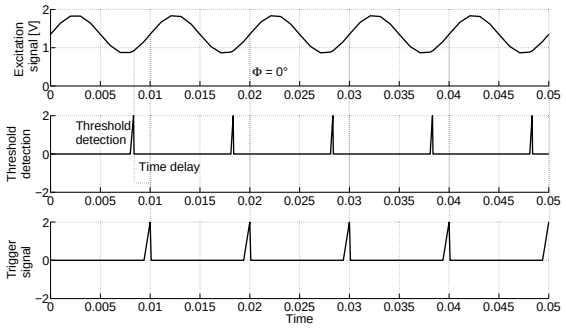

Figure 5: Timing diagram of the delay generator: An arbitrary time delay can be adjusted with reference to a voltage threshold[5]

For the reference case and the boundary-layer stabilization the PIV system consist of a conventional dual-cavity *Litron LP4550 laser* with a maximum repetition rate of 15 Hz and a wavelength of 532 *nm*, a single *Dantec FlowSense 2M* CCD camera, *Dantec 80X70* light sheet optics and a *Nikon AF Mikro Nikkor* 105*mm* lens. The cameras maximum resolution is 1600 x 1200 pixels, while only the upper sensor half is used. Seeding is introduced to the settling chamber with laskin nozzles, the droplets are provided by pressure vaporization of Di-Ethyl-Hexyl-Sebacat (DEHS), the resulting aerosol droplets have diamaters < 1 μm. The highest seeding density is found at the leading edge of the flat plate, to provide the boundary with sufficient particles, reaching an average value of 0.042 particles/pixel in the FOV. The PIV system operates in double frame mode at a repetition rate of 10 Hz. As a compromise of obtaining a high wall-normal resolution and capturing a whole TS wave length, the field of view was chosen to cover 33.4 *mm* in streamwise direction and $12,4$ *mm* in wall normal direction. The FOV was placed 60 *mm* downstream of the plasma actuator, because in this region the boundary-layer stabilization is expected to be distinctive. The minimum interrogation area (IA) size of 16 x 16 pixels with an overlap of 50 % was chosen, resulting in 199 x 71 interrogation areas. The conversion factor amounts to 48 $pixel/mm$, and the spatial resolution amounts to 8.53 IA/mm^2 without consideration of the 50% overlap. The dynamic spatial range (DSR) and the dynamic velocity range (DVR) are calculated according to Adrian [7] and amount to values of DSR=280 and DVR=294, respectively.

The accurate measurement of the velocities is crucial for this study, but it is difficult due to the large velocity gradients and small amplitudes of the TS wave. The accuracy of the velocity estimate obtained from the raw images will depend on the number of particles in the interrogation area as well as the exact estimator used to obtain the peak from the cross-correlation function. Therefore the time between the laser pulses in the consecutive frames has to be adjusted in a way, that ensures the optimal particle displacement of $1/4 - 3/4$ of an IA for the convective speed of the TS waves. According to Schlichting and Gersten [1] the convective speed of a TS wave in a laminar Blasius type boundary layer depends on its excitation frequency and the Reynolds number Re_δ based on the displacement thickness δ_1. For the given configuration (the Reynolds number Re_δ based on the displacement thickness δ_1 is $Re_\delta = 1160$ and the excitation frequency is $f_{ds} = 250$ Hz). Duchmann [8] calculates the convective speed of the TS waves U_{TS} using the linear stability theory to be $U_{TS} = 0.36U_\infty$. The wavelength of the TS waves can then be calculated to $\lambda_{TS} = U_{TS}/f_{ds} = 23.04$ *mm*, the FOV covers 140 % of a wavelength. Knowing the physical dimensions of the FOV and the convective speed of the TS waves, a time between the two frames of $T_f = 25$ μs is applied. For taking the large velocity gradient into account a multigrid correlation technique with successively downsized IA (from 64 x 64 pixels to 16 x 16 pixels) was used.

Two cameras setup - hybrid operation mode:

The measurement setup with two cameras is used to extend the FOV to about three TS wavelengths. This enables the amplitude of the TS waves upstream and downstream of the plasma actuator to be measured and to visualize the damping effect of the plasma actuator. Basically the setup consists of the same components as described in the section before. An additional Dantec FlowSense 2M CCD camera is mounted downstream of the other camera in order to extend the FOV in streamwise direction, which is 39mm for each camera. Due to the width of the lenses, both cameras are mounted side by side on Scheimpflug adapters. This allows a FOV overlap of 9mm in the streamwise direction. The dewarping and the interpolation of the images is described in section 2.6. The vibrating ribbon

as a disturbance source is replaced with a plasma actuator, driven by a Minipuls 0.1 from GBS Elektronik at an operating frequency of 9.8kHz. The operating voltage of the plasma actuator is amplitude modulated at 250Hz to excite the TS waves. Similar to the vibrating ribbon, the modulation signal is also used for triggering the data acquisition. Measurements in the near-wall region are difficult because reflections of the laser sheet at the wall can lead to erroneous data. To overcome this problem, a laser safety acrylic glass insert (Laservision 000P5E041012) is installed at the wall. This insert attenuates the laser light that enters the material and prevents reflection at the lower interface. This setup reduces the reflections significantly but the copper electrodes of the plasma actuator are still a source of reflections.

2.5 Data processing

Because the amplitude of the measured TS waves are very small (ca. 1% percent of the freestream), they can be easily masked by a slightly fluctuating wind tunnel velocity. The measurement uncertainty is given as 0.1 pixel by the manufacturer, which results in an uncertainty of 0.084 m/s for the given optics, which is of the order of magnitude of TS wave velocity deviations under the given conditions. The approach of the present study for all the measurement cases (reference case, boundary-layer stabilization, hybrid mode) is to average large enough ensembles to diminish the effect of stochastic velocity fluctuations on the recorded TS velocity deviations. An ensemble size of $N = 1700$ image pairs yields sufficiently converged statistics. The standard error under these conditions is 0.03 m/s in the boundary layer at a wall-normal distance of $y/\delta_{99} = 0.49$ and 0.019 m/s in the outer flow at a wall-normal distance of $y/\delta_{99} = 4.55$. The standard errors have been added to Figure 8 to illustrate their magnitude in comparison with the TS wave velocity deviations.
Extracting the velocity characteristics of the excited waves from the measured velocity fields requires data processing after the raw image pairs have been correlated. This data processing divides the acquired velocity fields into three classes. Each ensemble of velocity fields at a constant wave phase Φ is averaged and results in a mean velocity field $\overline{U}_\Phi$. The second class represents a velocity field without excitation: $\overline{U}$. This velocity field can be obtained by averaging all twelve velocity fields $\overline{U}_\Phi$. The effect of the excitation is canceled in $\overline{U}$, because $\overline{U}$ consists of twelve evenly distributed velocity fields. The third class represents the velocity deviations for a wave phase Φ from the mean velocity profile $\overline{U}$, which can be attributed to the excited wave: $\hat{u}_\Phi = \overline{U}_\Phi - \overline{U}$. The nomenclature for the wall-normal velocity component v is analoguous. The velocity deviations $\hat{u}_\Phi$ will be used to analyze the TS waves.
A Blasius type boundary layer is present in the FOV. The boundary-layer thickness obtained from the measurements is $\delta_{99} = 2.40$ mm, with a displacement thickness of $\delta_1 = 1.16$ mm. For TS waves there are typically two maxima of velocity deviations present, one with the higher magnitude inside the boundary layer, the other maximum outside of the boundary layer. Both are visible at their expected wall distances in the profile of $\hat{u}$ in Figure 8. In agreement with the linear stability theory the highest magnitudes of velocity deviations occur at $y/\delta_{99} = 0.37$ inside the boundary layer. The profile of velocity deviations is characteristic for TS waves.
An ensemble of twelve fields of TS velocity deviations $\hat{u}_\Phi$ represents a TS wave at twelve distinct phases Φ, i.e. twelve points in time. The periodicity of these ensembles can be used for a spectral analysis of the data. From such an analysis the spacial distribution of TS wave magnitude and phase can be obtained. This distribution is helpful when the different operational modes of the plasma actuator are characterized. The dampening effect can be quantified and be judged if the wave keeps its characteristic coherent structure after the actuation. The spectral analysis in form of a Fourier transformation is performed for each spatial point over phase angle Φ. Instead of using only one ensemble containing twelve distinct phases Φ, multiple ensembles are periodically concatenated into one record of 4096 repeating phases. Thus spectral broadening and the necessity of windowing can be eliminated and a Fast Fourier Transformation can be applied to the data. The result is an amplitude over frequency distribution at every interrogation area. Due to the image acquisition at fixed wave phases with a fundamental periodicity of $1/12$ 250 Hz, only frequencies of whole number multiples of the fundamental periodicity are expected. Figure 6 shows the spectrum of velocity deviations $\hat{u}_{150^\circ}$ inside the boundary layer at a wall distance of $y/\delta_{99} = 0.37$ and a position of $x/\lambda = 1.8$ downstream of the plasma actuator. The largest contribution to the velocity deviations from the base flow is due to the disturbance source operating at 250 Hz.

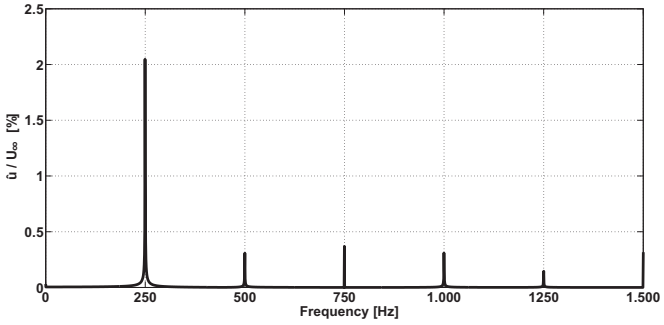

Figure 6: Spectrum of velocity deviations $\hat{u}$ inside the boundary layer at a characteristic position of $x/\lambda = 1.8$ and $y/\delta_{99} = 0.37$[5]

2.6 Two Camera Setup: Dewarping, Cross-Fading and Interpolation

The postprocessing of the velocity field acquired by the two cameras setup differs slightly from the description above, as two flow fields have to be dewarped and combined into one single grid.

Dewarping is necessary because of the angled view on the FOV of both cameras, as described in section 2.4. Hence a dot pattern calibration is carried out, showing a trapezoidal distortion of the images. It was discovered, that the integrated dewarping algorithm in the Dantec Dynamic Studio processing software leads to unsatisfying results, as the calculated dewarping grid exhibits small errors. These errors are negligible, if high velocity fluctuations are investigated. For TS wave measurements the error is in the same order as the TS wave fluctuations, therefore a new dewarping method is developed. The trapezoidal distortion is manually identified by measuring

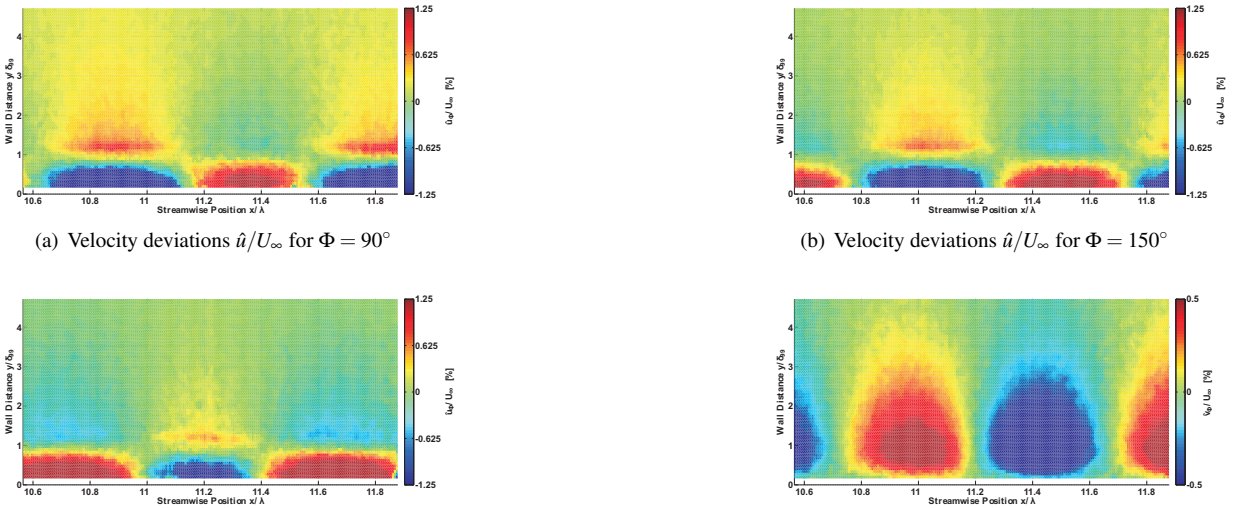

(a) Velocity deviations $\hat{u}/U_\infty$ for $\Phi = 90°$

(b) Velocity deviations $\hat{u}/U_\infty$ for $\Phi = 150°$

(c) Velocity deviations $\hat{u}/U_\infty$ for $\Phi = 210°$

(d) Velocity deviations $\hat{v}/U_\infty$ for $\Phi = 210°$

Figure 7: Normalized velocity deviations $\hat{u}/U_\infty$ and $\hat{v}/U_\infty$ for $\Phi = [90°150°210°]$[5]

the distance between the dots of the calibration targets, assuming a linear distortion in wall-normal and streamwise direction (viewing angle below 5°). After dewarping the velocity fields with this manual method, the results are verified by a constant mean flow velocity outside the boundary layer for the streamwise direction.

As both velocity fields have to be combined to a single grid, the overlapping regions are faded in and out with a linear function (cross-fading). Afterwards both velocity fields are linear interpolated to a new grid (400x100) as the grid points of each single velocity field are not adjusted to each other. The newly interpolated velocity field is then treated as described in the previous data processing procedure.

3. Results

This measurement procedure is applied to demonstrate the feasibility of resolving all relevant features of TS waves as they interact with a plasma actuator. For comparison, the reference case with deactivated plasma actuator, but with operating disturbance source is investigated. By comparing the results of this base line case to the case of the boundary-layer stabilization, the impact of the quasi-steady body force on the wave amplification and the boundary-layer stability can be quantified. The results also show the cancelation of the periodic disturbances when the plasma actuator is operated in hybrid mode.

3.1 Reference case

Important for the quantification of the interaction effect of a plasma actuator and TS waves is the resolution of the entire velocity fields of both velocity components $\hat{u}$ and $\hat{v}$. Figure 7a-c show these velocity fields for $\Phi = [90°150°210°]$, the mean flow direction is from left to right. Velocity deviations from the baseflow are indicated as blue (negative deviations) or red (positive deviations). It can be clearly seen that the pattern of velocity deviation is convected in the x direction with increasing Φ. A 180° phase shift in the vertical direction between spots inside and outside of the boundary layer is visible, which is characteristic for TS waves. Even the wall normal velocity deviations $\hat{v}$ can be resolved, as shown by Figure 7d. Again negative components of $\hat{v}$ appear blue and are directed toward the wall, positive ones appear red.

Furthermore, Figure 7 quantitatively shows the velocity distribution characteristic for TS waves: For $\hat{u}$ two maxima exist at $y/\delta_{99} \approx 0.37$ and $y/\delta_{99} \approx 1.30$. At $y/\delta_{99} \approx 0.92$ the velocity fluctuations are zero. The wavelength can be obtained directly from the periodicity of the velocity deviations $\hat{u}$ or $\hat{v}$. These values are in agreement with linear stability theory. In summary the results show the capability of the measurement method to resolve both velocity components of TS waves qualitatively and quantitatively. These results have been previously reported in [5].

Figure 8 shows a different visualization of the data: The shape of the TS velocity deviations $\hat{u}_{180°}$ in the reference case (Figure 8, black curves) is given as a function of the normalized wall-normal component y/δ_{99}. The amplitudes and positions of all distinctive points corresponds very well with the predictions of the linear stability theory.

3.2 Boundary-layer stabilization

In this section a quasi-steady body force is produced by the plasma actuator in order to stabilize the boundary layer. No active wave cancelation is conducted.

In contrast to the case of active wave cancelation the attenuation effect of the boundary-layer stabilization is not expected to occur immediately at the plasma actuator, where the body force is applied. The effect is distributed over some wavelengths downstream of the plasma actuator, since in this region the altered velocity profile exists and slowly decays. Figure 8 shows the the attenuation

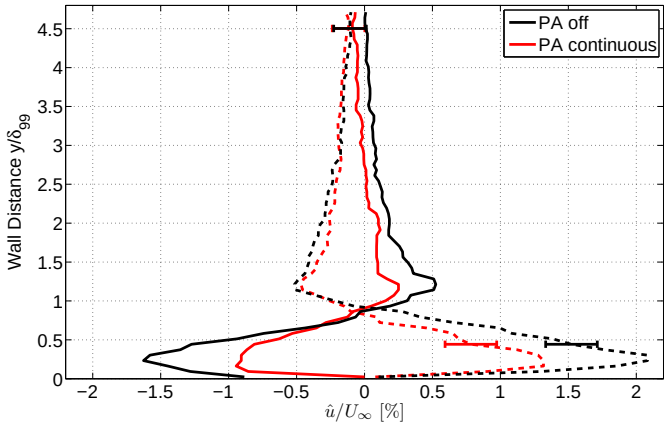

Figure 8: Velocity deviations $\hat{u}_{180}/U_\infty$ in the reference case (black curves) and $\hat{u}_{150}/U_\infty$ for the boundary-layer stabilization (red curve) as a function of non-dimensional wall distance y/δ_{99}. The dashed and the solid lines are shifted by a half wavelength in the downstream direction. The dampening effect is apparent in the reduced amplitudes of the velocity deviations $\hat{u}_{180}/U_\infty$.

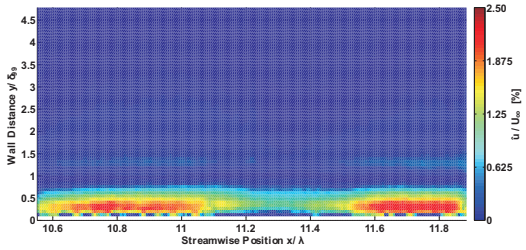

(a) Amplitude distribution $\hat{u}/U_\infty$ at 250 Hz for the reference case

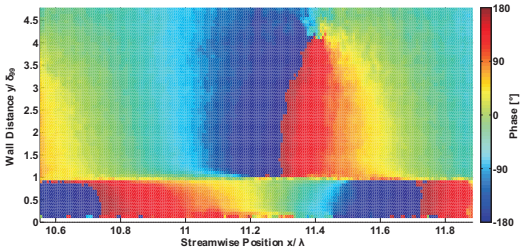

(b) Phase distribution $\hat{u}/U_\infty$ at 250 Hz for the reference case

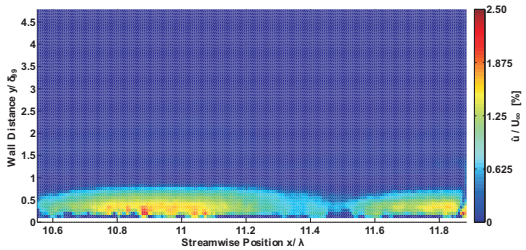

(c) Amplitude distribution $\hat{u}/U_\infty$ at 250 Hz for the boundary-layer stabilization

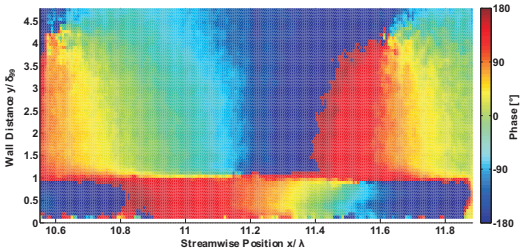

(d) Phase distribution $\hat{u}/U_\infty$ at 250 Hz for the boundary-layer stabilization

Figure 9: Comparison of the wall parallel amplitude distributions at a frequency of 250 Hz between the reference case and the boundary-layer stabilization

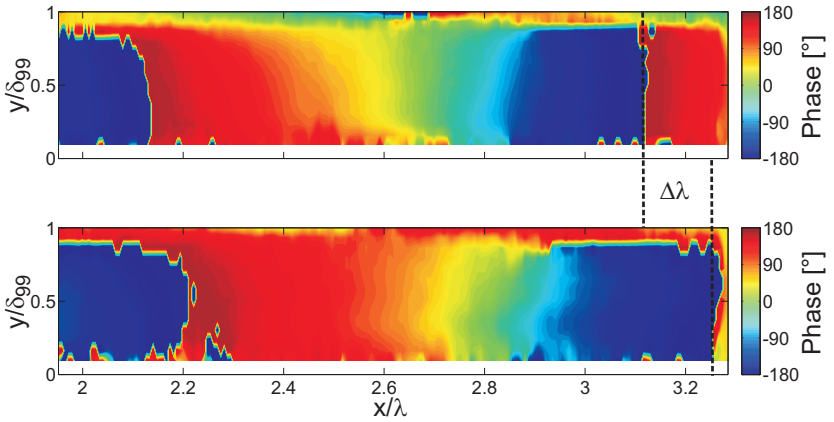

Figure 10: The comparison of the periodicity between the reference case and the boundary layer stabilization reveals an increased wavelength for the latter case

effect for the boundary-layer stabilization (red curve) as a reduction of the amplitudes of the velocity deviations, when compared to the reference case (black curve). To quantify the effect of the boundary-layer stabilization in terms of the magnitudes of the velocity deviations, a spectral analysis has been conducted. As shown by Figure 6 the most dominant velocity deviation can be found at a frequency of 250 Hz. The velocity deviations for this frequency are decomposed into a spacial amplitude distribution and a spacial phase distribution.

A comparison of the amplitudes $\hat{u}/U_\infty$ between the reference case and the boundary-layer stabilization is given in Figure 9(a) and (c). The amplitude distribution shows at which spatial position which velocity deviations occur. The largest velocity deviations occur inside the boundary layer. Outside the boundary layer a second maximum of lower magnitude can be seen. For $y \approx \delta_{99}$ the amplitude is approximately zero. These distinct points result in the typical amplitude distribution of TS waves.

It can be seen from the comparison of the reference case and the boundary-layer stabilization, that the amplification of the TS wave velocity deviations was reduced from 2.5 % to 1.5 % with respect to the free stream velocity, which corresponds to a reduction of approximately 40 %.

Figures 9 (b) and (c) show the phase distribution for the velocity deviations at an excitation frequency of 250 Hz. A strong periodicity is apparent in the phase distribution, which represents the wavelengths of the disturbances at a frequency of 250 Hz. At the wall-normal position between the two maxima of the wall-parallel velocity deviation a distinct 180 degree phase jump is clearly recognizable in wall-normal direction.

Another effect of the altered boundary layer properties can be seen from the comparison of phase distribution between reference case and boundary-layer stabilization: The convective speed of the waves is changed due to the body force, but the excitation frequency remains unchanged, which results in a varied wavelength. To show this more clearly the boundary-layer region is extracted from Figure 9(b) and (d) and presented in Figure 10. The difference of both wavelengths $\Delta\lambda$ (actuator on and off) is visible in Figure 10.

3.3 Hybrid Operation Mode

In this section an active wave cancelation using a modulated force with a constant offset for an additional stabilization is applied. This time a two camera setup is used. Figure 11(a) shows the reference case with artificial TS wave excitation. The growth of the velocity fluctuations in wall-normal direction along the horizontal coordinate is shown over more than two wavelengths. Earlier measurements with only one camera did not allow to measurements over a sufficient downstream distance.

The more interesting case is presented in Figure 11(b). It shows the development of the $\hat{v}$ component while the plasma actuator is operated in controlled hybrid operation mode. Obviously the wave amplitude is significantly reduced directly at the plasma actuator position $x/\lambda = 0$ due to the wave cancelation. The additional attenuation effect in the downstream region from the stabilization process is not as obvious in this FOV. The RMS value of the uncalibrated surface hot wire error sensor signal, which is located 40mm downstream of the plasma actuator, shows a drop of about 80% while the plasma actuator is operated in hybrid operation mode. Even if the signal is not calibrated and the maximum TS wave amplitude is not present directly at the wall, this order of magnitude for TS wave damping can also be observed for the wall-normal component $\hat{v}$. Due to the continuous body force, which is also added in the hybrid mode, a phase shift can also be seen, as described for the boundary-layer stabilization.

4. Conclusions and Outlook

The first conclusion of this study is that the phase-locked PIV technique is suitable for capturing and visualizing excited Tollmien-Schlichting waves in a laminar boundary layer. Moreover, the influence of a DBD plasma actuator, positioned for transition delay, can also be visualized. This is important, since due to electromagnetic disturbances associated with the actuators, few alternative methods are suitable. Capturing the entire flow field, over the entire boundary-layer thickness in the wall-normal direction, and over one or more

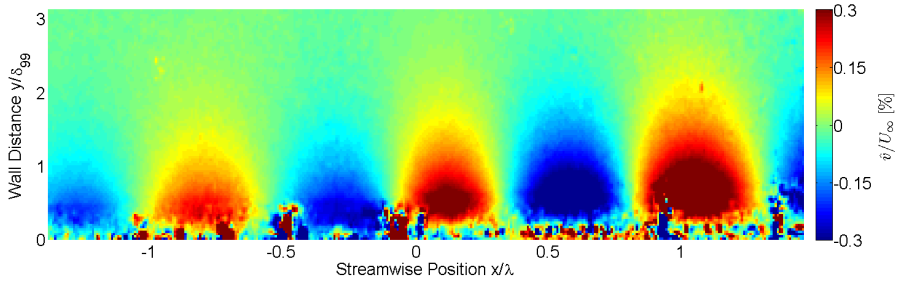

(a) TS Wave $\phi = 0°$.

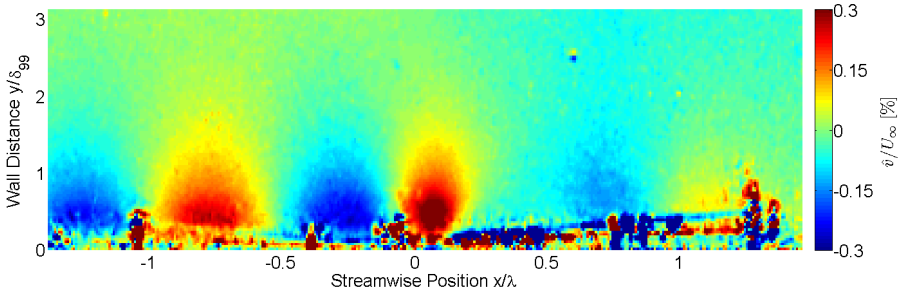

(b) Wave damping with hybrid operation mode.

Figure 11: Results of phase-locked PIV measurements with two cameras for hybrid operation mode

wavelengths of the TS-waves in the streamwise direction, allows the interaction between the DBD actuator and the TS-waves to be clearly seen. This interaction differs in nature depending on the operation mode of the actuators. In the boundary-layer stabilization mode, the TS-wave amplitude gradually decreases, since the velocity profile has been altered, such that it is no longer unstable to small perturbations. In the hybrid mode, acting directly in phase with the TS-wave disturbances, the TS-wave amplitude is suppressed almost completely directly at the actuator. These effects can be observed both in the U and V velocity components.

The information gained in this study is not only interesting for better understanding the actuator/TS-wave interaction, the measurements also offer data suitable for direct comparison with numerical simulations of the DBD plasma actuator. Integrating the actuator into numerical simulations of the boundary-layer transition requires a body force to be incorporated into the momentum equations as a source term. The magnitude, direction and spatial distribution of this force must be determined. The extent to which this body force is properly modeled can be evaluated by comparing the resulting velocity fields to data, such as that obtained in the present study. Hence, such measurements are a valuable addition to the overall understanding, design and application of plasma actuators for boundary-layer manipulation.

REFERENCES

[1] Schlichting H and Gersten K "Boundary Layer Theory" Springer 8 (2006)

[2] Grundmann S and Tropea C "Active Cancellation of Artificially Introduced Tollmien-Schlichting Waves Using Plasma Actuators" Experiments in Fluids 44 (2008) pp.795-806

[3] Grundmann S and Tropea C "Experimental damping of boundary-layer oscillations using DBD plasma actuators" Int J Heat Fluid Flow 30 (2009) pp.394-402

[4] Kurz A, Goldin N, King R, Tropea C and Grundmann S "Development of active wave cancellation using DBD plasma actuators for in-flight transition control" 6th AIAA Flow Control Conference, June 25-28 , New Orleans, USA (2012)

[5] Widmann A, Duchmann A, Kurz A, Grundmann S and Tropea C "Measuring Tollmien-Schlichting waves using phase-averaged particle image velocimetry" Experiments in Fluids 53 (2012) pp.707-715

[6] Baumann M "Aktive Dämpfung von Tollmien-Schlichting Wellen in einer Flügelgrenzschicht Fortschritt-Berichte VDI 7 VDI-Verlag Dsseldorf (1999)

[7] Adrian R J, "Dynamic ranges of velocity and spatial resolution of particle image velocimetry" Measurement Science and Technology 8 (12) (1997) pp. 1393-1398

[8] Duchmann A, Reeh A, Quadros R, Kriegseis J and Tropea C "Linear stability analysis for manipulated boundary-layer flows using plasma actuators" IUTAM Bookseries 18 (2009) pp.153-158